Electromagnetics, 30:574–588, 2010

ISSN: 0272-6343 print/1532-527X online
DOI: 10.1080/02726343.2010.513931

Adaptive Nulling with Time-Modulated Antenna Arrays Using a Hybrid Differential Evolution Strategy

YIKAI CHEN,[1] SHIWEN YANG,[1] GANG LI,[1] and ZAIPING NIE[1]

[1]Department of Microwave Engineering, School of Electronic Engineering, University of Electronic Science and Technology of China, Chengdu, P. R. China

Abstract *A flexible approach based on a hybrid differential evolution strategy was developed for adaptive pattern nulling with time-modulated linear antenna arrays. The hybrid differential evolution strategy adjusts only the least significant bits of the digital phase shifters and the on–off time sequence to minimize the total output power; deep nulls can then be placed in the direction of the interferences without much compromise of the shape of the main beam. Thanks to the new design freedom introduced in time-modulated antenna arrays, this adaptive nulling approach exhibits better performance over the traditional phase-only, amplitude-only, and phase-amplitude adaptive nulling methods, in terms of the practical implementation, nulling depth, and pattern deterioration. Numerical examples are presented to demonstrate the effectiveness and robustness of the proposed approach.*

Keywords antenna arrays, adaptive nulling algorithm, time modulation, differential evolution

1. Introduction

The use of adaptive antenna arrays in electronic communication systems can be dated back to late 1960s. Adaptive arrays that are used in the polluted electromagnetic environment are aimed at separating a desired signal from interfering ones. Common adaptive algorithms, such as the Applebaum adaptive processor, provide the mathematical basis for the optimization of signal-to-interference plus noise ratio (SINR) in the presence of interference sources and background noise (Applebaum, 1976). However, the Applebaum approach requires the full inversion of the sampled covariance matrix, and it is not a trivial task to get the sampled covariance matrix, both from the view point of the hardware implementation and the algorithmic standpoint (Haupt, 1997). Although alternative approaches, such as the least mean square (LMS) and recursive least square (RLS) algorithms, have been proposed to avoid the matrix inversion (Pokrajac et al., 2001), the inherent drawbacks in such methods prohibit their widespread use. In more detail, LMS and RMS require analog amplitude and phase weights at each element;

Received 1 August 2009; accepted 15 December 2009.
Address correspondence to Shiwen Yang, Department of Microwave Engineering, School of Electronic Engineering, University of Electronic Science and Technology of China (UESTC), Chengdu, 610054, P. R. China. E-mail: swnyang@uestc.edu.cn

although the use of variable amplitude weights is very desirable from a theoretical point of view, the implementation of amplitude control is extremely costly and is rarely used in practical systems. For this reason, adaptive arrays usually adopt digital phase shifters only but with the loss of the full control of the antenna patterns.

In order to exploit the existing capability of phased arrays for the purpose of mitigating electromagnetic interference without extra cost, another class of phase-only adaptive nulling algorithms has been studied extensively in recent years (Haupt & Shore, 1984; Haupt, 1988, 1997, 2006; Chung & Haupt, 1999; Steyskal et al., 1986). This class of algorithm usually adjusts only the least significant bits (LSB) of digital phase shifters for the reduction of the total output power. Haupt and Shore (1984) presented the experimental results to demonstrate the practicality of the phase-only adaptive nulling methods in existing phased arrays, where the adaptive nulling method was performed by minimizing the total array output power using the gradient search algorithm without significant deteriorations in the main beam shape.

Various adaptive nulling methods based on full amplitude-phase control at each array element and methods with a restricted number of degrees of freedom have been discussed to illustrate their merits and limitations. Unlike the phase-only method, the amplitude-phase control method adjust both the amplitude and phase excitations in the adaptive process; thus, the degrees of freedom are increased. From a theoretical point of view, the adaptive nulling can be realized more easily due to the increased degrees of freedom, but it is also the most costly method as compared to other methods such as the amplitude-only or phase-only methods. A trade-off exists between the quality of the constrained pattern and the complexity of electronic control (Steyskal et al., 1986). A method based on the gradient search algorithm was presented in Haupt (1988) for the phase-only adaptive nulling in a monopulse antenna. In this method, the gradient search algorithm adjusts the adaptive phase weight settings to simultaneously search for a minimum in the sum and difference channel output powers. Both theoretical and experimental results demonstrate that this algorithm is capable of placing deep nulls in the direction of interference, despite the algorithm seeming nearsighted and slow.

A real-time application of the genetic algorithm (GA) for the phase-only adaptive nulling was presented in Haupt (1997). In the GA-based phase-only adaptive nulling method, some of the LSB of the beam steering phase shifters are adjusted to minimize the total array output power; thus, the deviation in the beam steering direction and perturbation in the side-lobe levels (SLLs) are rather small, while nulls can be placed in the direction of interference precisely and quickly. The GA-based adaptive nulling method was then extended to spherical arrays (Chung & Haupt, 1999), where the LSB of the amplitude weight bits were controlled as well as the phase shifters to minimize the total output power, and the deteriorations in the main beam were also rather limited. The studies of Haupt (2006) showed how the restricted degrees of freedom allow the GA-based adaptive nulling method to minimize the total output power to reject the interference while at the same time not leading to a large perturbation in the far-field pattern.

All the aforementioned studies showed that the adaptive nulling method with variable amplitude and phase is the most efficient method; however, previous studies on phase-only adaptive nulling methods have also indicated that amplitude control in adaptive nulling is not normally considered as a viable option, both for their high cost and the difficulties in the hardware implementation; thus, the phase-only adaptive nulling method deserves much interest. On the other hand, the time-modulated antenna arrays, which have regained their research interests for array designs with critical amplitude requirements, are generally considered an alternative to overcome the difficult amplitude control problem in conventional antenna arrays (Yang et al., 2003, 2005a, 2005b; Yang & Nie, 2006, 2007; Fondevila et al., 2004; Chen et al., 2008a). The previous works on time-modulation antenna arrays mainly focus on the pattern synthesis problems, and the time-modulated antenna array is only taken as an alternative of the traditional antenna array for typical applications. However, no work has been done to make the time-modulated antenna array applicable to smart antenna systems, such as adaptive nulling. Moreover, adaptive beamforming methods can be rather sensitive to steering vector errors and frequency variations, and the time-modulation technique can provide high precision in the control of amplitude excitations in a convenience way. Thus, application of the time-modulated antenna arrays to the adaptive pattern nulling problems for the enhancement of robustness becomes the motivation of this study.

This article presents a flexible adaptive nulling approach based on hybrid differential evolution strategy (HDES; Caorsi et al., 2005; Chen et al., 2008b). It possesses the capability of excellent control over the array pattern in amplitude-phase methods. A number of simulation results are presented to investigate the performance of the method from various aspects. Several representative examples are presented to show the effectiveness of the proposed method.

2. The Adaptive Nulling Approach for Time-Modulated Antenna Arrays

2.1. Model of the Time-Modulated Antenna Array

A $2N$-element linear array with $\sin\phi$ element patterns lying along the x-axis (Figure 1) is considered. Each element is controlled by a high-speed radio frequency (RF) switch and is weighted with a static complex factor $A_n e^{j\alpha_n}$ $(n = 1, 2, \ldots, 2N)$. The static complex weights are assumed to be symmetrical about the array center, and the phase reference point is taken at the center of the array. If a plane wave of frequency f_0 is incident at an angle ϕ with respect to the endfire of the array, the normalized output signal from the array can be expressed as

$$E(\phi, t) = \sin\phi e^{j2\pi f_0 t} \sum_{n=1}^{2N} A_n e^{j\alpha_n} U_n(t) e^{j(n-N-0.5)\beta d \cos\phi}, \quad (1)$$

where d is the element spacing, $\beta = 2\pi f_0/c$, c is the velocity of light in free space, and $U_n(t)$ $(n = 1, 2, \ldots, 2N)$ represents the periodic switch on–off time function in which each element is switched on for τ_n $(0 \leq \tau_n \leq T_p)$ in one modulation period T_p by the high-speed RF switch (Yang et al., 2003, 2005a, 2005b; Yang & Nie, 2006, 2007). The complex programmable logical device (CPLD) is used for the time sequence generator, which quickly and precisely controls the on–off time of the high-speed RF switches, thus ensuring the physical realization of the adapted "time" weights. The pulse repetition frequency $f_p = 1/T_p$ is usually much lower than the carrier frequency f_0. Since arrays weighted with uniform amplitude are easier and less expensive for the practical summation network implementation, uniform amplitude weights ($A_n = 1$) are employed throughout this study. The element pattern $\sin\phi$ is the approximation of radiation patterns of antennas such as dipoles lying along the y-axis.

By defining and expanding the output signal in Eq. (1) into a Fourier series with different frequency components $f_0 + mf_p$ ($m = 0, \pm 1, \ldots, \pm\infty$), the mth-order Fourier

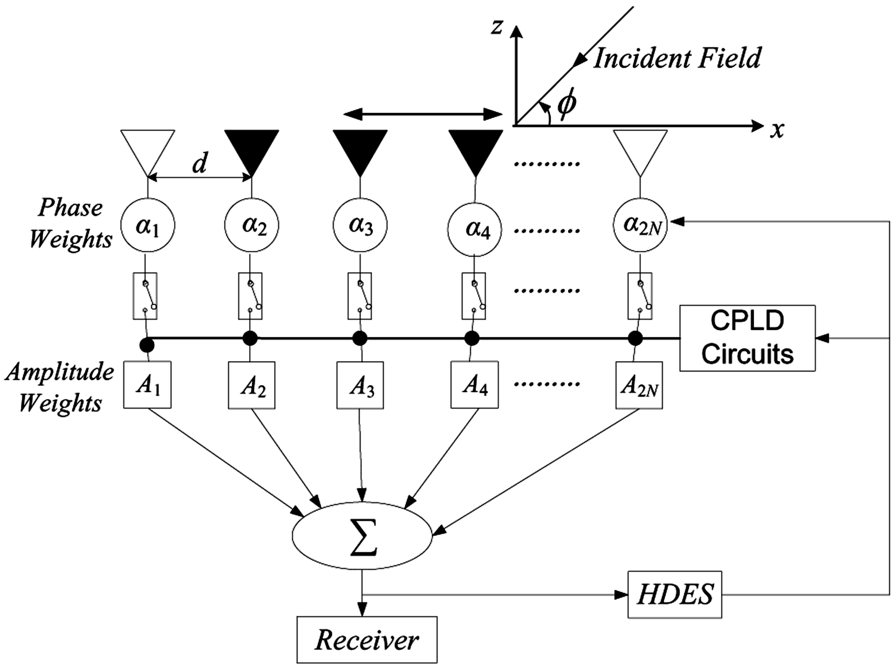

Figure 1. Diagram of an adaptive time modulated antenna array controlled by HDES.

component of Eq. (1) is given by

$$E_m(\phi) = \sin\phi \sum_{n=1}^{2N} w_n^{(m)} e^{j(n-N-0.5)\beta d \cos\phi}, \tag{2}$$

where $w_n^{(m)}$ is the equivalent weights of element n for the mth harmonic component and is given by

$$w_n^{(m)} = e^{j\alpha_n} \frac{\tau_n}{T_p} \cdot \frac{\sin(m\pi f_p \tau_n)}{m\pi f_p \tau_n} \cdot e^{-jm\pi f_p \tau_n}. \tag{3}$$

It is known from Eq. (3) that although uniform amplitude weights are employed, the equivalent amplitude weights at the center frequency f_0 ($m = 0$) can be well adjusted by altering the on–off time sequence $U_n(t)$. Thus, the excellent pattern control capability of amplitude control methods is retained while the difficulty in the amplitude control is eliminated.

In order to perform beam steering and adaptive pattern nulling with the same phase shifter settings, the static phase weights α_n ($n = 1, 2, \ldots, 2N$) are decomposed into phase φ_n for beam steering and phase δ_n for nulling, as the main beam is steered to an angle of $\phi_{\max}$, measured from the endfire of the array. The static phase weight α_n can be represented as

$$\alpha_n = \varphi_n + \delta_n = -(n - N - 0.5)\beta d \cos\phi_{\max} + \delta_n. \tag{4}$$

φ_n, as well as δ_n, are quantized in an array with digital phase shifters; it differs from $-(n - N - 0.5)\beta d \cos\phi_{\max}$ and must be represented as its quantized counterpart Δ_n.

When the adaptive nulling method is applied in a phased array, phase Δ_n is determined first to steer the beam to a proper angle, and the phase for nulling will be adjusted jointly with the on–off time sequence using the method introduced next.

2.2. The Adaptive Nulling Approach

Any adaptive nulling method proposed is to enhance the reception of the desired signal and reject the interferences. Since the desired signal is always mixed with the interferences, minimizing the total output power will also minimize the desired signal unless the desired signal is assumed to enter the main beam and there is no null placed in the main beam. Another case is that if there is no interference, the desired signal will be minimized directly; thus, the degeneration of the desired signal is an important practical topic and should be paid great attention. To prevent the desired signal degeneration, the adaptive nulling approach is based on an HDES, where some LSB of the digital phase shifters and small values of perturbations imposed on the on–off time weights τ_n are taken as the optimization parameters. These variable settings have a small effect on the main beam but can place nulls in the side-lobes.

For any commercially available digitized phase shifters that control the phase excitation of each antenna element, it is feasible to assume that the least P significant bits are taken as the adjustable nulling phase in a digital phase shifter with B bits ($P < B$); the nulling phase is then represented by

$$\delta_n = 2\pi \sum_{i=0}^{P-1} b_i 2^{-(B-i)}, \tag{5}$$

where b_i is the binary bits defined for the representation of δ_n. It is known from Eq. (5) that the nulling phases can only take digitalized values for the digital phase shifters, and these digitalized values are varied with a minimum value of $2\pi/2^B$. The on–off time weights τ_n, which serve as another degree of freedom for the adaptive pattern nulling, are assigned with a small perturbation range of $[-\Delta_\tau, \Delta_\tau]$. Obviously, the search range of the perturbations imposed on τ_n is a continuous space, due to the fact that the on–off time of a high-speed RF switch control can be negligibly small as compared to the modulation period T_p. On the other hand, the search range of the nulling phase is in a discrete space; thus, the HDES is employed to deal with optimization problems with a hybrid of both continuous and discrete optimization parameters (Caorsi et al., 2005; Chen et al., 2008b).

Similar to the GA, the differential evolution strategy (DES) proposed by Storn and Price (1997) also belongs to the class of population-based optimization methods. The DES has been proven to be an excellent optimizer for engineering problems with continuous search space (Qing, 2003, 2006; Chen et al., 2007); however, applications of the DES in problems with discrete search space or hybrid search space has rarely been studied (Caorsi et al., 2005; Chen et al., 2008b). In order to deal with problems with both continuous and discrete optimization parameters, the HDES is employed in this article. In order to take profit from the powerful search ability of the DES in the continuous search space, each chromosome in the HDES population consists of the perturbations imposed on τ_n and continuous phase values in the search space of the digitized phases. The evolution mechanism remains the same as those in the DES. The main difference between the DES and the HDES is that as the evolution procedure proceeds, the continuous phase values in each chromosome are approximated by their nearest digitized phase values; these digitized phase values are then employed for the calculation of the cost function, but the continuous perturbations imposed on τ_n are directly used for the cost function computation. The modifications introduced in the DES have also been introduced into the the HDES optimization solver to enhance the convergence rate and exploration ability (Chen et al., 2008b).

For convenience, a vector $\boldsymbol{v} = [\Delta_{\tau n}, \delta_n]$ is defined to denote all the optimization parameters involved in the adaptive nulling method, where $\Delta_{\tau n}$ is the perturbation superimposed on the on–off time weight τ_n at the nth array element. Since the adaptive nulling method is based on the minimization of the total output power from the array, the cost function in the HDES optimization should contain the output power term. In adaptive nulling problems with conventional antenna arrays, the total output power term is immediately taken as the cost function. However, in the time-modulated antenna arrays considered here, nulls are only required to be placed in the array pattern at the center frequency f_0 ($m = 0$); thus, only the output power at the center frequency serves as the term in the cost function for the purpose of array pattern nulling. On the other hand, considering the inherent drawback that there are sideband radiations ($m \neq 0$) in time-modulated arrays (Yang et al., 2002), part of the radiated power is shifted to the sidebands. In order to enhance the radiation efficiency, the sideband radiations should be suppressed by adding the corresponding term into the cost function, just as in the array pattern synthesis problems (Yang et al., 2002). The construction of cost function is rather flexible; the only requirement for the cost function is that it can minimize the total output power as well as the sideband radiations—no other restrictions are required. Therefore, in order to place nulls adaptively and suppress the sideband radiations in the adaptive nulling approach, the following cost function is constructed and applied throughout this article:

$$f(\boldsymbol{v}) = \eta_1 \cdot 20\log_{10}\left\{\sum_{i=1}^{N_I+1} s_i \sin\phi_i \left|\sum_{n=1}^{2N} w_n^{(0)} e^{j(n-N-0.5)\beta d\cos\phi_i}\right|\right\}$$
$$+ \eta_2 \cdot \frac{SBL_{\max}(\boldsymbol{v})}{SBL_0} U[SBL_{\max}(\boldsymbol{v}) - SBL_0]\bigg|_{m\neq 0}, \tag{6}$$

where

$w_n^{(0)} = e^{j(\delta_n+\Delta_n)}\frac{\tau_n+\Delta_{\tau n}}{T_p}$ is the adjusted weight at the nth element, and the first term in Eq. (6) represents the total noncoherent output power at the center frequency;

η_k ($k = 1, 2$) is the weighting factor of each term to emphasize the different contributions to the cost function;

s_i represents the signal strength of source i;

ϕ_i is the incident angle of source i;

$N_I + 1$ is the number of signal sources, including one desired signal and N_I interfering sources, which correspond to a practical situation, where both the desired signal as well as the interference signals are presented;

U is a Heaviside step function, and the second term in Eq. (6) represents the relative error of the sideband level (SBL) $SBL_{\max}(\boldsymbol{v})$ with respect to the desired level SBL_0.

In Eq. (6), it is assumed that the incident angles of the interferences and desired signal are different. In the case when the interference incident is in the same direction as that of the desired signal, null will be placed in the incident angle of the desired signal, and the desired signal will not be received. The reason behind this fact is that the adaptive process is only based on the total output power of the array, and the power of the desired signal will also be minimized if interferences are mixed in the same incident angle. Numerical results will be presented that demonstrate the rationality of this assumption.

Figure 1 shows the diagram of a time-modulated adaptive array controlled by the HDES. The HDES starts by initializing the population randomly with a uniform probability distribution. New nulling chromosomes are generated from old ones, and chromosomes with lower cost function values are kept, while those large values are discarded; thus, the output power at the center frequency and the peak levels of the radiation pattern at the first sideband $f_0 + f_p$ (which is normally the maximum SBL; Chen et al., 2008a) should be measured for each chromosome. However, both the DES (Storn & Price, 1997) and the MDES (Chen et al., 2008b) have a large population size (usually three to five times the number of optimization parameters) to ensure that the optimum can be found successfully; the large population size will slow the algorithm immediately and make the algorithm not suitable for real-time application like adaptive nulling. On the other hand, a crucial requirement for the adaptive nulling method is that the algorithm should be fast, but a global minimum is not necessary since a −50-dB null can reject an interference as well as a −90-dB null does. From this point of view, a relatively small population is used in the HDES to accelerate the nulling speed, but the small population selected should also be large enough to keep the search out of local minima.

3. Numerical Results and Discussion

In this section, the behavior of the HDES-based adaptive nulling method in time-modulated antenna arrays is studied. The effectiveness of the adaptive nulling method is first demonstrated, and the robustness of the method is investigated by concerning various simulated interference scenarios.

3.1. A General Demonstration for the Effectiveness of the Method

In order to show the capabilities of the adaptive nulling method, a 40-element time-modulated linear array with a −30-dB Chebyshev pattern at the center frequency is modeled. The time-modulation period T_p is 1 μs, implying a pulse repetition frequency of $f_p = 1$ MHz. The equivalent amplitude taper at the center frequency is formed from a tapered on–off time sequence, and uniform static amplitude weights are employed to avoid the difficult static amplitude tapering. Elements are spaced $0.5\lambda_0$ apart at the center frequency $f_0 = 1.56$ GHz; the phase shifters have six-bit accuracy, and only the two least significant bits are taken as the adaptive nulling phase. The perturbations on the on–off time weights should be small enough to avoid significant main bean deterioration.

On the other hand, the perturbations should be large enough to facilitate the pattern nulling. Thus, the search range of the perturbations to be imposed on the on–off time weights τ_n is set to be $[-0.23T_p, 0.23T_p]$, which is a suitable range to compromise the two factors. Two interfering sources are assumed to appear at $u = 0.62$ and 0.72, each 60 dB stronger than the desired signal power, where $u = \cos\phi$ is the cosine space coordinate. The incident angles of the two interferences are the locations of two of the side-lobe peaks of the −30-dB Chebyshev pattern. In fact, this problem has been studied in conventional antenna arrays (Haupt, 1997). The quiescent and adapted array patterns at f_0 and the first two sidebands are plotted in Figures 2 and 3, respectively. As can be seen from Figure 3, nulls deeper than −50 dB are created in the pattern at the center frequency, and the distortion brought to the main beam is rather small with an increased SLL of −27 dB. This improved SLL over that obtained by Haupt (1997) is benefited

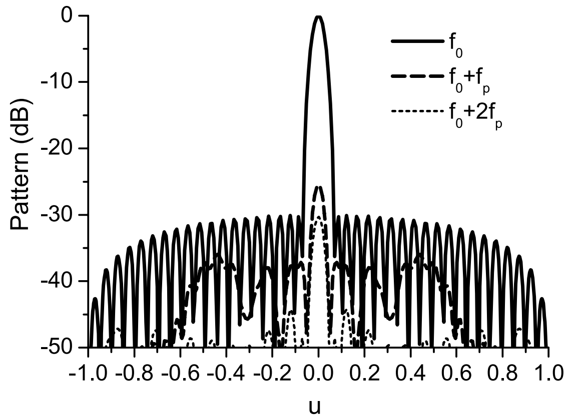

Figure 2. The quiescent time-modulated antenna array patterns with a −30-dB Chebyshev pattern at the center frequency.

from the additional degrees of freedom in time-modulated arrays. The maximum SBL was suppressed to −16.7 dB. Convergence of the algorithm is shown in Figure 4; it can be observed that about 250 power measurements are required for the nulls forming in the two interference directions. Since the number of optimization parameters has been doubled as compared to the phase-only nulling method, and another term has been included in the cost function for SBL suppression, the convergence speed of the optimization algorithm is lowered immediately, leading to a larger number of power measurements than those in phase-only methods (Haupt, 1997).

As a fair comparison for the adaptive nulling speed, the same time-modulated antenna array has been considered, whereas the term for SBL suppression is not included in the cost function. The resulting adapted pattern and convergence rate are shown in Figures 5 and 6, respectively. It is noted that the maximum SBL goes up to about −12 dB, due to the exclusion of the SBL suppression term in the cost function. It can also be observed that only 70 power measurements are needed for the null forming, which indicates that the efficiency of the adaptive nulling method proposed herein is the same

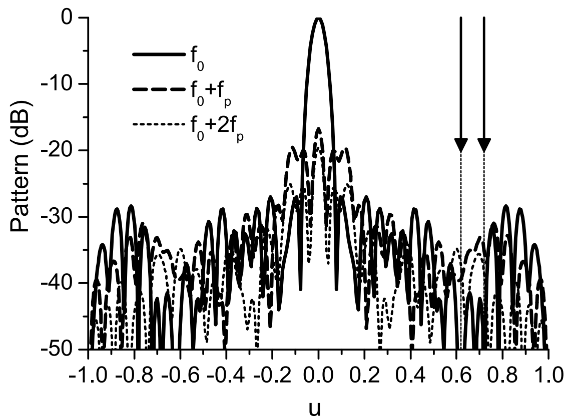

Figure 3. The adapted time-modulated antenna array patterns with sideband suppression.

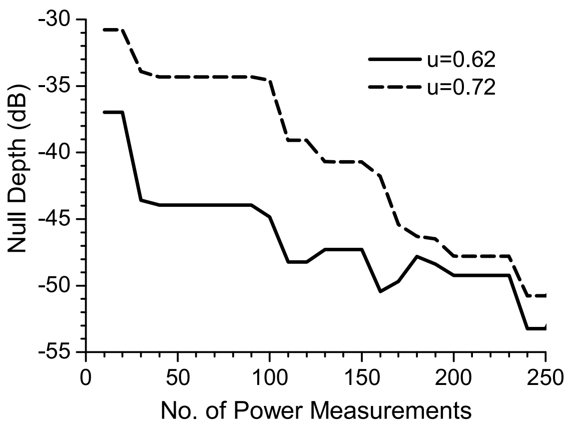

Figure 4. Null depth as a function of the number of power measurements.

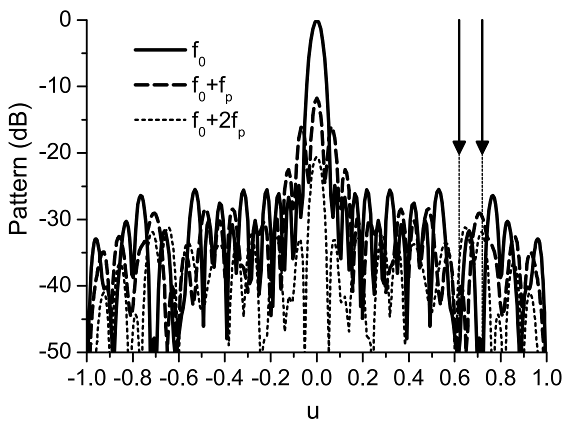

Figure 5. The adapted time-modulated antenna array patterns without sideband suppression.

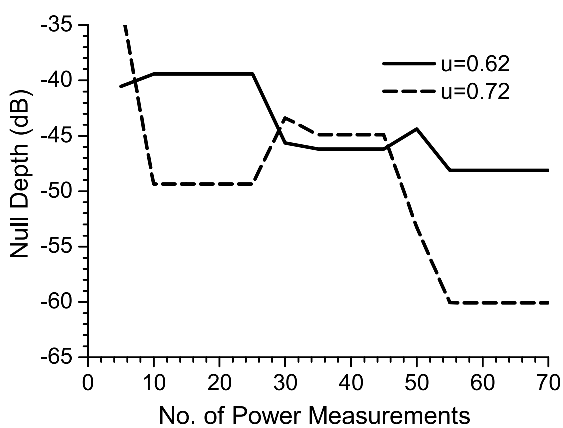

Figure 6. Null depth as a function of the number of power measurements.

as the phase-only adaptive nulling method based on the GA (Haupt, 1997), despite that the number of optimization parameters is doubled due to the new degrees of freedom introduced. Moreover, thanks to the new degrees of freedom in time-modulated antenna arrays, the resulting SLL of the pattern at f_0 (about −25 dB) is lower than that obtained by Haupt (1997). To this end, it can be observed that the pattern distortion can be reduced through the introduction of the time-modulation technique, and the convergence rate of the adaptive nulling method can be improved largely if the sideband radiations are not considered. Fortunately, the sideband radiations and the pattern at f_0 are different in frequency; thus, the sideband radiations can be filtered out at the intermediate frequency (IF) band. Even so, it is strongly recommended that the sideband radiations should be suppressed if only the signal at the center frequency is needed, partly for the reason that the convergence rate in the sideband suppression case is still in the acceptable range.

3.2. Investigations on the Performance of the Method

In order to provide a comprehensive insight into the HDES-based adaptive nulling method in time-modulated antenna arrays, results from various interference scenarios are presented, and discussions on the effectiveness and robustness of the adaptive algorithm then follow.

First, the impact of the number of nulling phase bits P on the performance of the adaptive nulling methods is investigated. The same adaptive time-modulated antenna array in the above example is considered, but the number of nulling phase bits P is varied from three to five. Figure 7 shows the adapted patterns and the corresponding convergence rate for the $P = 3$, 4, and 5 cases. It can be seen that the deterioration in the main beam is rather small when three nulling phase bits are used, and the adapted pattern for $P = 3$ is similar to the adapted pattern for $P = 2$ (Figure 3). However, in the $P = 4$ and 5 cases, the maximum SLL goes beyond −25 dB, and at the same time the main beam width is broadened. Therefore, it is reasonable to conclude that smaller phase perturbation leads to a relatively modest pattern perturbation, while larger phase perturbations will deteriorate the main beam significantly. Moreover, by comparing the convergence rate curves in Figure 7(b) with those shown in Figure 4 and Figure 6 for the $P = 2$ case, it is observed that a larger number of nulling phase bits will lower the convergence rate. Because of the relatively small population size applied in the HDES optimization algorithm and the larger search space, the search for the optimal optimization vector $\boldsymbol{v}$ becomes rather difficult for the HDES. Thus, it is also reasonable to conclude that a small number of nulling phase bits is more suitable in this type of adaptive nulling method with respect to the convergence rate and the distortion caused in the main beam.

Second, the robustness of the adaptive nulling method is investigated by considering whether a null can be created in the vicinity of the main beam. This investigation is based on a 100-element time-modulated array with uniform equivalent weights at the center frequency $f_0 = 1.56$ GHz; the time modulation period is also set to be $T_p = 1$ μs. The interference in the main beam vicinity is located at $u = 0.03$, with a strength 54 dB stronger than the desired signal. The second interfering source is located at $u = 0.73$ and is 46 dB stronger than the desired one. Here, the simulated adaptive antenna array is, in fact, the same as that considered in Haupt (1997); the only difference is that the time-modulation technique has been introduced in the present model. It has been suggested by Steyskal et al. (1986) that large phase perturbations are required in phase-only methods when a null is imposed in the vicinity of the main beam. Thus, four LSB are used for the forming of nulls in this high side-lobe array. The search range for the perturbations

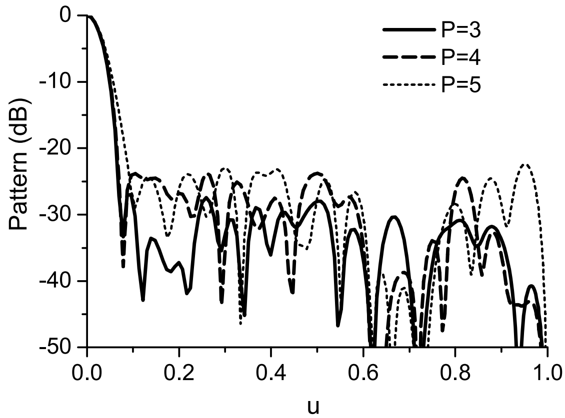

(a)

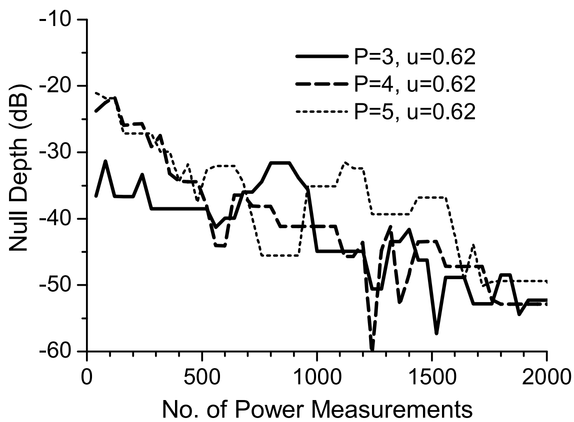

(b)

Figure 7. Impact of the nulling phase bits on the performance of the adaptive nulling algorithm: (a) adapted patterns for various numbers of nulling phase bits; (b) null depth versus the number of power measurements for various numbers of nulling phase bits.

imposed on the on–off time weights is also set to be $[-0.23T_p, 0.23T_p]$. Figure 8 plots the nulled pattern and the patterns at the first sideband. It can be seen that two nulls are placed precisely in the direction of the interferences; the null created at $u = 0.03$ is 5 dB deeper than that obtained by Haupt (1997), and this deeper null is also benefited from the time-modulation technique. Moreover, due to the additional degree of design freedom, the SLL obtained here is about -17.5 dB, which is also lower than that in Haupt (1997). The maximum SBL was suppressed to -20 dB, which is a sufficiently small SBL for the reduction of the inherent power loss in the time-modulation technique. Therefore, the adaptive nulling algorithm is capable of placing nulls in the vicinity of the main beam.

Third, the robustness of the adaptive nulling method is also investigated by changing the strength of the interference signal. The same adaptive time-modulated antenna array in the section entitled "A General Demonstration for the Effectiveness of the Method" is

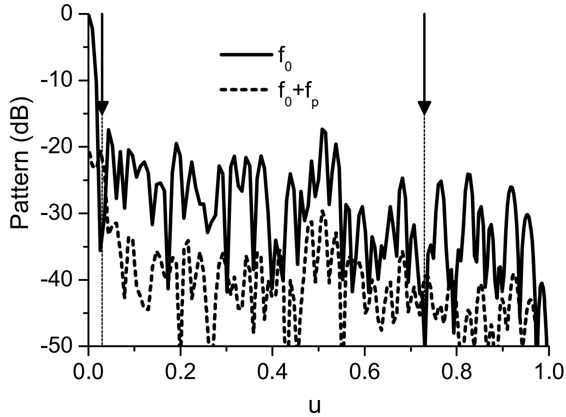

Figure 8. The adapted array patterns for the rejection of interference in the main beam vicinity.

considered. The number of nulling phase bits is chosen as $P = 2$, and various interference scenarios of a strong interfering source (SIR) equal to -50 dB, -20 dB, and 10 dB are considered. The resulting adapted patterns corresponding to different interference scenarios are presented in Figure 9. It shows that this adaptive nulling algorithm is more suitable for the rejection of a low SIR, since more serious deterioration will appear in the main beam as the SIR increases. Through simulations, it has also been found that the convergence rate will also be lowered in large SIR cases. Moreover, it can be observed from Figure 9 that nulls cannot be placed effectively when the SIR increases beyond 0 dB.

Fourth, the robustness of the adaptive nulling method is investigated by increasing the number of the interference sources. Each of the interference sources is assumed to be 60 dB stronger than the desired signal. The incident angle of the desired signal is still assumed to be at $u = 0$, and the sideband radiations have not been suppressed in this case. Figure 10 shows the adapted patterns when eight interferences with incident angles of $u = 0.22$, 0.32, 0.42, 0.52, 0.62, 0.72, 0.82, and 0.92 are presented. It can be observed that the adapted pattern in Figure 10 has almost the same SLL as those in the case with two interferences, although the number of interferences has been increased

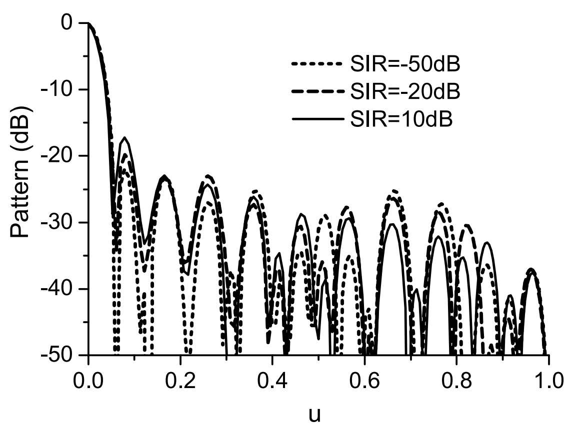

Figure 9. The adapted time-modulated antenna array patterns for various SIRs.

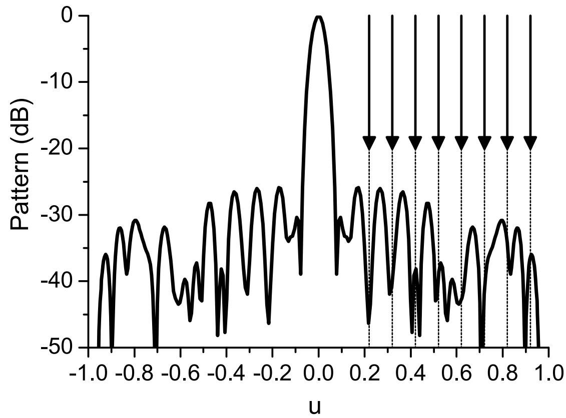

Figure 10. Adapted pattern of the time-modulated antenna array when eight interferences are presented.

greatly. The average null depth over the eight interference incident angles is -39.8 dB, with a maximum value of -34.25 dB and a minimum value of -46.35 dB. Therefore, the adaptive nulling method also has the capability of adaptive nulling in a complicated electromagnetic environment. On the other hand, it is necessary to point out that the number of interferences is also restricted by the "freedom" of the antenna array, where the maximum number of nulls created by any adaptive nulling method cannot exceed $2N - 1$ (Compton, 1988).

Finally, the strength of the method is demonstrated by investigating the output signal-to-interference ratio from the time-modulated adaptive antenna array. The same time modulated linear array with 40 elements is considered. It is assumed that two continuous waves are incident on the array—one is the desired signal, and the other is the interference. Let the desired signal and the interference arrive from incident angles of u_d and u_i, respectively, and also assume that the interference is 60 dB stronger than the desired. The incident angle of the desired signal is always assumed to arrive at $u_d = 0$, which is also the normal direction of the array axis. The perturbations to be imposed on the on–off time weights τ_n is set to be $[-0.23T_p, 0.23T_p]$, and the least $P = 3$ significant bits are taken as the phase perturbations. Figure 11 shows the output SIR from the array as a function of the incident angle of the interference, where u_i is increased from -1.0 to 1.0 with a step of $\Delta u_i = 0.02$. It can be seen that the SIR drops dramatically when u_i is near $u_d = 0$, since the desired signal falls in the interference null. As $|u_i - u_d| > 0.06$, the SIR is improved to be greater than 0 dB, and the SIR is over 10 dB for most incident angles. It implies that the desired signal can be received successfully while the interference signal is rejected, as long as the arrival angles of the two signals are not close to each other.

4. Summary and Conclusion

This article presented an adaptive nulling method in time-modulated antenna arrays. An HDES was employed to deal with such kinds of problems with both continuous and discrete optimization parameters. Numerical results show that with the introduction of the time-modulation technique in adaptive nulling arrays, the excellent pattern control

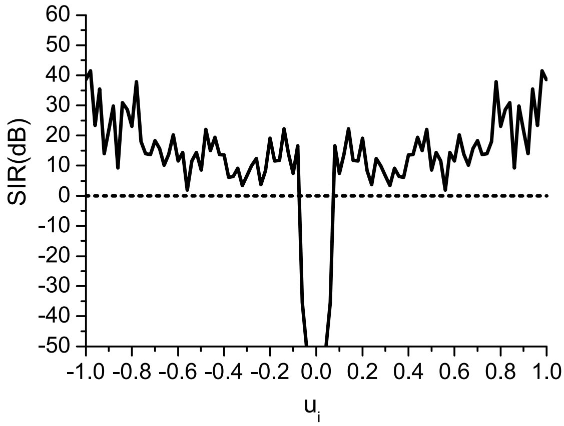

Figure 11. Output SIR of the time-modulated antenna array for interferences with different arrival angles.

capability inherent in amplitude-phase nulling methods is retained, but the difficulty in the amplitude control technique is eliminated. The contribution of this article also rests with the complete performance investigation from various aspects, many of which are rarely discussed since the proposal of the adaptive nulling method. Based on these numerical experiments, characteristics of the proposed adaptive nulling method were summarized, including both their advantages and their limitations. The characteristics of the adaptive nulling algorithm are summarized below.

1) Information of the interfering sources (including the directions and strengths) is not necessary.
2) The adaptive array can be constructed from the existing time-modulated antenna array without extra costs.
3) The adaptive algorithm is more suitable for the rejection of stronger interferences.
4) It is a fast adaptive nulling algorithm and can be used in real time applications.
5) Thanks to the new degrees of freedom introduced in the time-modulated antenna array, the main beam deterioration becomes less serious, and deeper nulls can be created.
6) Small phase perturbations are preferred, due to the small population size used in the HDES.
7) The adaptive algorithm has the ability to reject interferences at the vicinity of the main beam.
8) Since only the noncoherent output power is included in the cost function, the adaptive algorithm only has the ability to reject noncoherent interferences.
9) If the sideband suppression is not considered, the nulling speed remains the same as in the traditional phase-only nulling methods; even the number of optimization parameters is doubled.

Acknowledgments

This work was supported by the Natural Science Foundation of China (grant 60571023), the New Century Excellent Talent Program in China (grant NCET-06-0809), and was also partially supported by the 111 project of China (grant B07046).

References

Applebaum, S. P. 1976. Adaptive arrays. *IEEE Trans. Antennas Propagat.* AP-24:585–598.

Caorsi, S., A. Massa, M. Pastorino, & A. Randazzo. 2005. Optimization of the difference patterns for monopulse antennas by a hybrid real/integer-coded differential evolution method. *IEEE Trans. Antennas Propagat.* AP-53:372–376.

Chen, Y., S. Yang, & Z. Nie. 2007. Synthesis of uniform amplitude thinned linear phased arrays using the differential evolution algorithm. *Electromagnetics* 27:287–297.

Chen, Y., S. Yang, & Z. Nie. 2008a. Synthesis of satellite footprint patterns from time modulated planar arrays with very low dynamic range ratios. *Int. J. Numer. Model.* 21:493–506.

Chen, Y., S. Yang, & Z. Nie. 2008b. The application of a modified differential evolution strategy to some array pattern synthesis problems. *IEEE Trans. Antennas Propagat.* AP-56:1919–1927.

Chung, Y. C., & R. L. Haupt. 1999. Adaptive nulling with spherical arrays using a genetic algorithm. *Proc. IEEE AP-S Int. Symp. Dig.* 3:2000–2003.

Compton, R. T. 1988. *Adaptive antennas: concepts and performance*. Englewood Cliffs, NJ: Prentice-Hall.

Fondevila, J., J. C. Brégains, F. Ares, & E. Moreno. 2004. Optimizing uniformly excited linear arrays through time modulation. *IEEE Antennas Wirel. Propag. Lett.* 3:298–301.

Haupt, R. L. 1988. Adaptive nulling in monopulse antennas. *IEEE Trans. Antennas Propagat.* AP-36:202–208.

Haupt, R. L. 1997. Phase-only adaptive nulling with a genetic algorithm. *IEEE Trans. Antennas Propagat.* AP-45:1009–1015.

Haupt, R. L. 2006. Adaptive antenna arrays using a genetic algorithm. *2006 IEEE Mountain Workshop on Adaptive and Learning Systems*, Logan, UT, 24–26 July, 249–254.

Haupt, R. L., & R. A. Shore. 1984. Experimental partially adaptive nulling in a low sidelobe phased array. *Proc. IEEE AP-S Int. Symp. Dig.* 2:823–826.

Pokrajac, I., M. Sunjevaric, & B. Zrnic. 2001. The base station antenna array system output SINR determination for different spatial channel models. *Proc. 5th TELSIKS* I:141–144.

Qing, A. 2003. Electromagnetic inverse scattering of multiple two-dimensional perfectly conducting objects by the differential evolution strategy. *IEEE Trans. Antennas Propagat.* AP-51:1251–1262.

Qing, A. 2006. Dynamic differential evolution strategy and applications in electromagnetic inverse scattering problems. *IEEE Trans. Geosci. Remote Sens.* 44:116–125.

Steyskal, H., R. A. Shore, & R. L. Haupt. 1986. Methods for null control and their effects on the radiation pattern. *IEEE Trans. Antennas Propagat.* AP-34:404–409.

Storn, R., & K. Price. 1997. Differential evolution—a simple and efficient heuristic for global optimization over continuous spaces. *J. Global Optim.* 11:341–359.

Yang, S., Y. B. Gan, & A. Qing. 2002. Sideband suppression in time-modulated linear arrays by the differential evolution algorithm. *IEEE Antennas Wirel. Propag. Lett.* 1:173–175.

Yang, S., Y. B. Gan, A. Qing, & P. K. Tan. 2005a. Design of a uniform amplitude time modulated linear array with optimized time sequences. *IEEE Trans. Antennas Propag.* AP-53:2337–2339.

Yang, S., Y. B. Gan, & P. K. Tan. 2005b. Linear antenna arrays with bidirectional phase center motion. *IEEE Trans. Antennas. Propagat.* 53:1829–1835.

Yang, S., Y. B. Gan, & P. K. Tan. 2003. A new technique for power pattern synthesis in time modulated linear arrays. *IEEE Antennas Wirel. Propag. Lett.* 2:285–287.

Yang, S., & Z. Nie. 2006. The four dimensional linear antenna arrays. *The 2006 Fourth Asia-Pacific Conference on Environmental Electromagnetics*, Dalian, China, 1–4 August, 692–695.

Yang, S., & Z. Nie. 2007. Millimeter-wave low sidelobe time modulated linear arrays with uniform amplitude excitations. *Intl. J. Infrared Millmeter. Waves* 28:531–540.